



## **EXPERIMENTAL VERIFICATION OF A GENERIC BUFFETING LOAD MODEL FOR HIGH-RISE AND LONG-SPAN STRUCTURES**

Robin G. SROUJI, Kristoffer HOFFMANN

Svend Ole Hansen ApS, Denmark

[rgs@sohansen.dk](mailto:rgs@sohansen.dk), [kho@sohansen.dk](mailto:kho@sohansen.dk)

Svend Ole HANSEN

SOH Wind Engineering LLC, USA

[soh@sohansen.dk](mailto:soh@sohansen.dk)

### **INTRODUCTION**

Frequency-based aerodynamic admittance functions are key elements in the modelling of buffeting loads on structures exposed to natural winds. For wind-sensitive structures, such as tall slender buildings or long-span bridges, wind tunnel experiments are often used as a procedure for identifying the structural buffeting characteristics. For instance, in section model testing with bridge decks, spatial limitations associated with model-scale experiments imply that very little information is obtained about the pressure correlation along the main dimension of the structure, making it difficult to predict the full-scale behavior of the bridge. A common approach is therefore to predict the full-scale buffeting load from an experimentally determined cross-sectional aerodynamic admittance function combined with conservative assumptions of the normalized co-spectrum of the forces along the main structural dimension. Full-scale buffeting load predictions based on results from model-scale experiments with high-rise structures exhibit similar challenges.

A recent paper by the authors above [1] introduced a stochastic buffeting lift prediction procedure, which reduced uncertainties considerably by applying a more physical consistent description of the pressure correlations along bridge decks. This newly introduced buffeting load model has a generic form and therefore encompass the fields of building and bridge engineering in a single mathematical framework straightforward to codify. Actual differences between surface pressure characteristics at various parts of the structure are accounted for in the proposed framework.

Accurate and physically consistent predictions of buffeting loads require fundamental knowledge of the interaction between the wind field, the generated surface pressures and the net wind load. This involves the use of quantities modelling the associated variations in frequency characteristics and reduced spatial and temporal correlation. The present paper addresses such fundamental investigations of structure-induced upstream surface pressure characteristics, based on a series of wind tunnel experiments.

## Aerodynamic admittance - theory

Aerodynamic admittance is a frequency-based measure of the ratio between the generated surface pressures and the fluctuating amplitudes in the undisturbed wind, and this is a key element for accurate and physically consistent predictions of buffeting loads. Naturally, this requires fundamental knowledge of the interaction between the wind field and the generated surface pressures for a given structure.

On a point-like structure, the power spectrum of the pressure may be modelled by the simplified relation [2]

$$S_p(n) = (\rho U)^2 S_u(n), \quad (1)$$

where  $\rho$  is the air density,  $U$  the mean wind velocity, and  $S_u(n)$  the power spectrum of the undisturbed along-wind velocity.

For structures that are not point-like, the fluctuating pressure field on the upstream surface is different. In the high-frequency range, the fluctuating wind components are increasingly incapable of producing a fluctuating surface pressure similar to that of a point-like structure. This characteristic is expressed by the aerodynamic admittance function

$$\chi^2(n) := \frac{S_p(n)}{(\rho U)^2 S_u(n)}, \quad (2)$$

modelling the frequency-based relative reduction in fluctuating amplitudes, when the along-wind turbulence is converted to associated surface pressure fluctuations. Note that this relation does not consider the lack of spatial correlation of pressures on the upstream structural surface, but is modelling the point-wise structure-induced pressure fluctuation smoothing at high frequencies. In other words, the aerodynamic admittance expresses the ability of a fluctuating wind velocity to produce fluctuating surface pressures on a given structure, defined relative to a quasi-static setting.

Typical engineering structures enforce surface pressures and associated wind load characteristics, which may be estimated with an acceptable precision by codified formula in relevant building codes. Since codified formula are naturally calibrated against such typical and traditional structures, they encapsulate characteristics associated with typical structural dimensions. The estimation of wind loads on non-typical structures, such a high-rise or long-span constructions therefore have to be treated with caution to ensure that the key physical characteristics responsible for the associated mean and buffeting loads are included in the modelling framework.

One of the main motivations for the present work is to investigate at which frequencies that the aforementioned effect is initiated, as modelled by the aerodynamic admittance function. This may be especially relevant for high-rise or long-span structures, where such structure-induced effects should impose a significant net load reduction even for small fluctuation frequencies, due to the large spatial dimensions, and this is of particular interest in connection with the resonant wind actions at the natural frequency. As it will be shown, this effect is related to the spatial dimensions of the structure, and therefore the aerodynamic admittance function is in the following modelled as a function of the reduced frequency  $nh/U$ , which is an expression of the ratio relevant geometrical dimension  $h$  and the wavelength  $U/n$ , which again is a ratio between the mean wind velocity and a given frequency.

## Correlation of wind turbulence and surface pressure fluctuations

Structures with typical geometrical dimensions are often found capable of producing a distinct correlated fluctuating pressure field on the upstream surface, manifested by a net surface pressure correlation larger than that of the approaching wind. On the other hand, very large structures are generally not capable of producing such an effect on the complete surface, and the net surface pressure characteristics are found to be more similar to the correlation characteristics of the approaching wind.

This dissimilarity is closely linked to the ratio between the spatial extension of the structure and the integral length scale of along-wind turbulence.

A commonly used approach, is to model the spatial correlation of along-wind turbulence components based on a simple empirical exponential formula for the normalized co-spectrum

$$\psi_u(r, n) = \exp\left(-\frac{Crn}{U}\right), \quad (3)$$

where  $r$  is the separation distance and  $C$  a decay constant. This format was originally proposed by Davenport [3].

The format above incorporates at least two inconsistencies, which are in violation with basic physical principles. Firstly, a strictly positive correlation is obtained for any spatial separation, leading to a non-zero mean turbulence component in the plane perpendicular to the wind direction. Secondly, the format prescribes full correlation at low-frequency components, even for very large separations, which is impossible due to the spatial limitations of naturally occurring vortices. These two inconsistencies make the simple exponential format unsuitable for the estimation of relevant wind loads for high-rise and long-span structures, where an accurate co-spectra description for large spatial separations is crucial.

The observations mentioned above have motivated the formulation of a modified exponential format, which does not suffer from similar physical inconsistencies [4]. In the two-dimensional form, the spatial coherence function for the along-wind turbulence components takes the form

$$\psi_u(r_y, r_z, n) = \left(1 - \frac{1}{2} \frac{n_x}{U} \sqrt{(C_y r_y)^2 + (C_z r_z)^2}\right) \exp\left(-\frac{n_x}{U} \sqrt{(C_y r_y)^2 + (C_z r_z)^2}\right), \quad (4)$$

for lateral and vertical separations,  $r_y$  and  $r_z$ , and associated decay constants,  $C_y$  and  $C_z$ . The modified frequency  $n_x$  is defined as

$$n_x := \sqrt{n^2 + \left(\frac{U}{2\pi L}\right)^2}, \quad (5)$$

where the length scale  $L$  is derived from a generalized form of the von Kármán spectrum, and incorporates the effect of reduced correlation for low-frequency components, even at large spatial separations [2].

In the second part of the experimental campaign, the spatial correlation of the incoming wind and the surface pressures are investigated and compared to the modified exponential format presented above. The experiments are primarily related to model structures imposing two-dimensional flow, similar to the flow setting around high-rise and long-span constructions, and includes a model relation where only lateral separations are considered.

## EXPERIMENTAL PROCEDURE

Two general model structures, representing general types of structure-induced upstream surface pressure characteristics, are considered in the conducted wind tunnel experiments. These two general model types cover fundamental structures typically considered in engineering design, and are denoted point-like and slender structures.

The concepts of point-like and slender structures are associated with the spatial dimensions of the upstream structural surface compared to the size of vortices in the approaching wind at the frequencies considered. Slender structures have a single dimension of the same order of magnitude or larger than the integral length scale of along-wind turbulence, and one dimension which is comparable to or smaller, while for point-like structures both dimensions are much smaller than the length scale.

## Model structures

Pressure measurements have been conducted on two main types of nominally rigid model structures, namely cubic point-like model structures and slender model structures. The slender model structures consist of three model structures with a square cross section and two model structures with a rectangular cross section. The geometrical dimensions and the location of the pressure taps on the upstream surface may be seen in Figure 1. All the model structures are positioned centrally in the wind tunnel, i.e. the flow may stream above and beneath the models. The undisturbed wind has been measured in the empty wind tunnel at similar locations using dual-sensor X-wire probes.

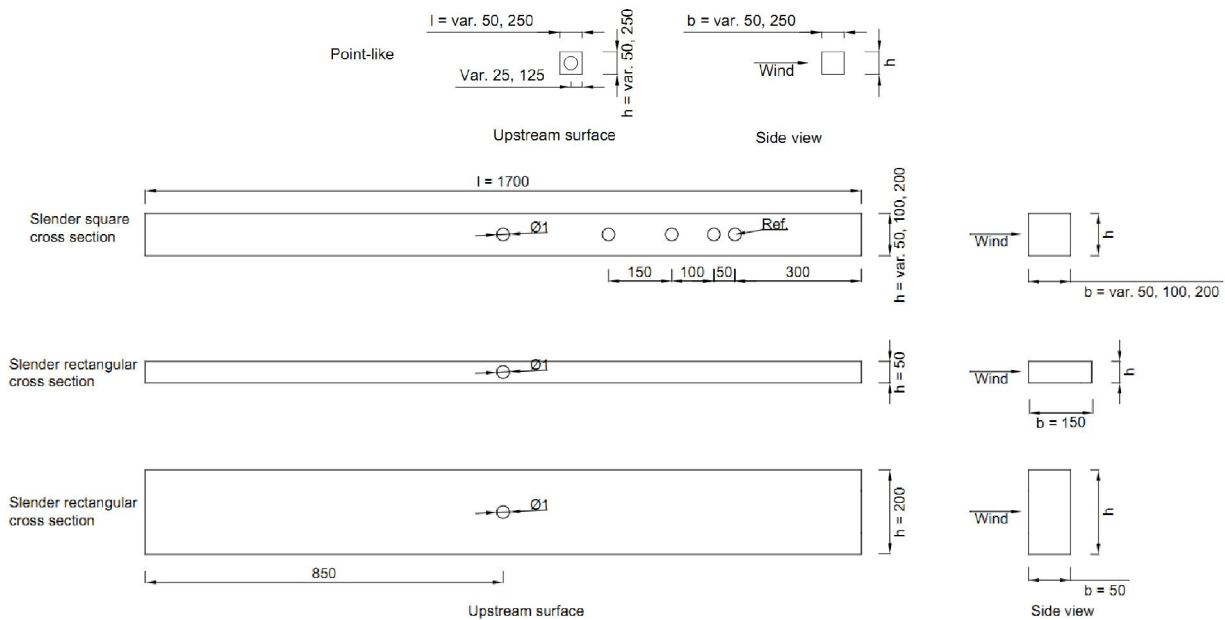


Figure 1. Pressure tap locations on the upstream surface of the investigated model structure types. The pressure taps are placed at mid height. The cross section of each model structure is a square. All the model structures are positioned centrally in the wind tunnel. The pressure taps have a diameter of 1 mm. All dimensions are in [mm].

As an example of a slender high-rise structure, the CAARC building has also been investigated on a scale 1:400; see Figure 2. The CAARC building model was placed on the wind tunnel floor.

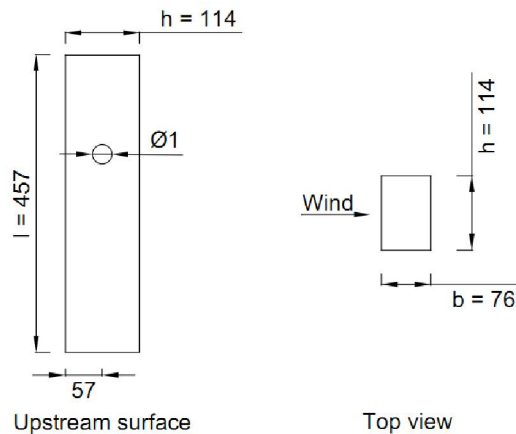


Figure 2. Pressure tap locations on the upstream surface of the CAARC building model. The pressure taps have a diameter of 1 mm. All dimensions are in [mm].

The frequency-based transfer function between longitudinal turbulence components of the undisturbed wind field and the corresponding surface pressure fluctuations, i.e. the aerodynamic admittance functions, is evaluated at the lateral center of the model.

The lateral spatial correlation of wind turbulence and surface pressure fluctuations have only been evaluated on the slender square cross sections with  $h = b = 5$  and  $10$  cm.

The tests were performed in turbulent flow with along-wind horizontal and vertical turbulence intensities of approx. 13-15 % and 7-9 %, respectively. Some tests have been carried with slightly different turbulence intensities. This may be seen on the figures in the result section. The sample frequency was at least 500 Hz, and the wind velocity was approx. 8 m/s.

### **Wind tunnel and flow characteristics**

All presented experiments have been conducted using nominally rigid pressure-tapped model structures in the boundary layer wind tunnel facility located at Svend Ole Hansen ApS in Copenhagen, Denmark and at SOH Wind Engineering LLC. The wind tunnel cross section at Svend Ole Hansen ApS has a height of 1.50 m and a width of 1.75 m. The wind tunnel cross section at SOH Wind Engineering LLC has a height of 3.0 m and a width of 3.0 m.

Characterizing the flow components of the undisturbed wind is the natural starting point for the presented buffeting load analysis. Correlations on upstream surfaces are related to the spectral and temporal characteristics of the longitudinal flow components, separated in the lateral or vertical dimension for the chosen wind tunnel environment.

## **EXPERIMENTAL RESULTS AND DISCUSSION**

The performed experiments illustrate the qualitative relationship between the geometry of an upstream surface and the associated surface pressure characteristics.

### **Wind characteristics**

The integral length scale of turbulence is a measure of the average size of the turbulence eddies. There are three integral length scales of turbulence associated with each of the longitudinal, lateral, and vertical fluctuating velocity components, namely  $u$ ,  $v$ , and  $w$ , respectively.

Several methods may be used to determine the size of the integral length scale. In the present paper, the fluctuation of the along-wind and cross-wind components have been described by the power spectral density function after von Kármán [5]; see Figure 3 and Figure 4, respectively. This produced the following estimated integral length scales:  $L_u^x = 0.50$  m and  $L_w^x = 0.14$  m. Some tests have been carried with slightly different length scales. This may be seen on the figures in the result section.

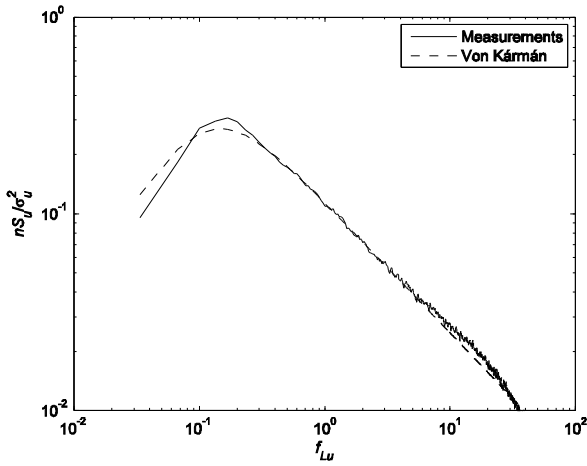


Figure 3.  $nS_u/\sigma_u^2$  – Non-dimensional power spectral density of the longitudinal turbulence component  $u$ .

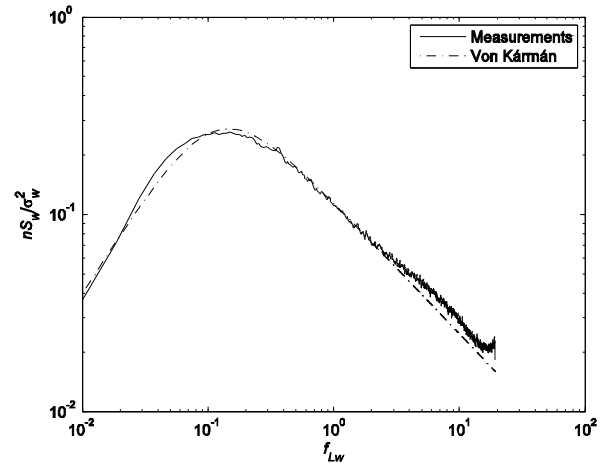


Figure 4.  $nS_w/\sigma_w^2$  – Non-dimensional power spectral density of the vertical turbulence component  $w$ .

Note that the ratio  $L_u^x/L_w^x$  in natural winds is normally found to be approximately twice the ratio obtained from the values of the above length scales. This discrepancy may be caused by the spatial limitations of the wind tunnel environment reducing low-frequency vortices, corresponding to a decrease in  $L_u^x$ .

### Aerodynamic admittance - measurements

The aerodynamic admittance functions for the slender and point-like structure types are presented in Figure 5 through Figure 7.

Figure 5 reveal that in a two-dimensional flow setting, similar to a structure having one very large dimension compared to the length scale, a decay of the aerodynamic admittance functions commence at a non-dimensional frequency  $nh/U$  of approx.  $10^{-1}$ . This may imply that as the dimension  $h$  perpendicular to the main structural axis is reduced, the net effect of aerodynamic admittance is gradually limited to larger frequency components. Accordingly, a profound effect from the aerodynamic admittance is not to be expected on structures with very small dimensions perpendicular to the main structural axis compared to the length scale. However, one should note that for the model structure of  $5 \times 5 \times 170$  cm, the slightly less steep decay of the aerodynamic admittance function may partially be caused by spectral folding effects associated with a finite sampling rate. The spectral folding occurs at lower non-dimensional frequencies as the dimension perpendicular to the main structural axis, used in the non-dimensional frequency, is reduced.

Along with the effect of the geometrical dimensions compared to the length scale, the results may also indicate that the Strouhal number  $St$  could be associated with the aerodynamic admittance function. The Strouhal number is related to vortex-induced vibrations, which mainly occur on slender structures, and is described similarly to the non-dimensional frequency when the vortex shedding frequency coincide with an eigenfrequency of a structure. What is noteworthy in Figure 5 is that for all the investigated slender model structures, the decay of the aerodynamic admittance function commence at the non-dimensional frequency of  $10^{-1}$ , which may correspond to the Strouhal number of 0.10. For slender structures with square cross sections, the Strouhal number typically lie within 0.08 and 0.12 [6,7]. This could indicate some sort of correlation between the periodic vortex formation on the alternate sides of the slender model structures, the bifurcation of the flow at the stagnation point, and the aerodynamic admittance function.

The influence of the Strouhal number on the aerodynamic admittance function is further strengthened by the results acquired from the investigations of the rectangular model structures  $h \times b \times l = 5 \times 15 \times 170$  cm and  $20 \times 5 \times 170$  cm; see Figure 6. For the  $h \times b \times l = 5 \times 15 \times 170$  cm model structure, the decay of the aerodynamic admittance function is observed at approx.  $7 \times 10^{-2}$ , while the decay of

the aerodynamic admittance function for the  $h \times b \times l = 20 \times 5 \times 170$  cm model structure takes place slightly above  $10^{-1}$ . These values correspond to Strouhal numbers of approx. 0.07 and 0.10, respectively. The change of the Strouhal number complies with the Eurocode 1 specifications of the Strouhal number dependency on sharp-edged structures [7]; see Figure 8. These findings will need further investigation for a full comprehension.

The aerodynamic admittance derived from the upstream surface pressures of the analyzed  $5 \times 5 \times 5$  cm point-like model structure shown in Figure 7 is found to be approximately unity, giving the relatively small spatial dimensions compared to the relevant length scales. Increasing the dimensions of the point-like model structure to dimensions comparable to the relevant length scales of  $25 \times 25 \times 25$  cm produce a reduction of the aerodynamic admittance function from unity. It should be noted that the measurements for the  $25 \times 25 \times 25$  cm model structure were carried out with a slightly different turbulence intensity and length scale than for the  $5 \times 5 \times 5$  cm model structure. However, the overall results indicate that aerodynamic admittance is an effect, which is significant only for two structural dimensions larger than, or at least comparable to, relevant length scales of the wind turbulence.

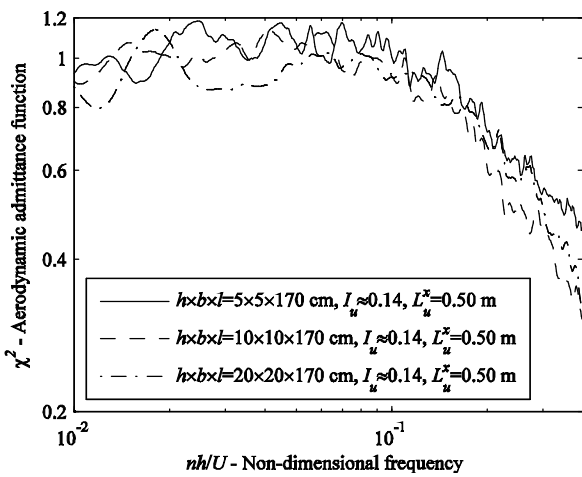


Figure 5. Aerodynamic admittance function for slender structure with  $h \times b \times l = 5 \times 5 \times 170$  cm,  $10 \times 10 \times 170$  cm, and  $20 \times 20 \times 170$  cm.

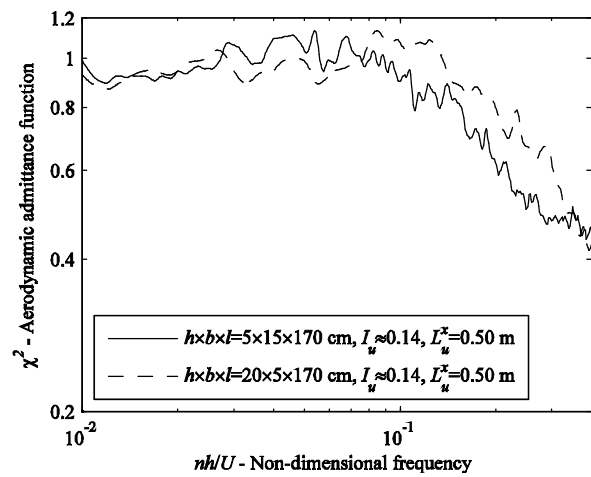


Figure 6. Aerodynamic admittance function for slender structures with  $h \times b \times l = 5 \times 15 \times 170$  cm and  $20 \times 5 \times 170$  cm.

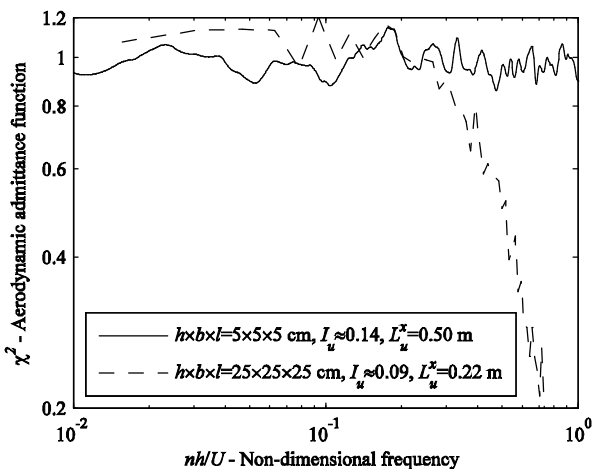


Figure 7. Aerodynamic admittance function for cubic structures with  $h \times b \times l = 5 \times 5 \times 5$  cm and  $25 \times 25 \times 25$  cm. Note that the abscissae is different from Figure 5 and Figure 6.

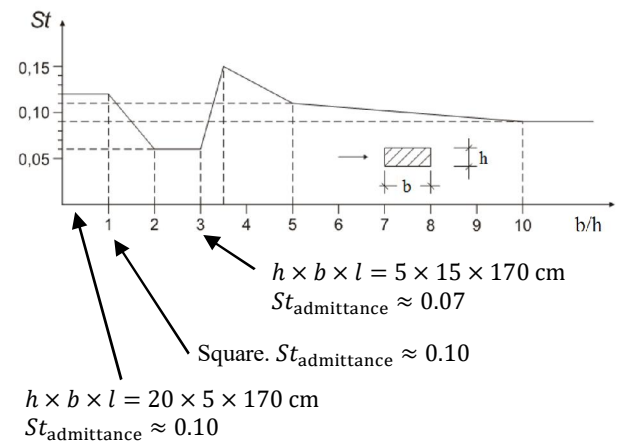


Figure 8. Variation of Strouhal number for different cross sections with sharp edges [7].

The aerodynamic admittance function for the CAARC building may be seen in Figure 9. The figure reveals similar tendencies as it was seen for the slender model structures in Figure 5, i.e. a decay of the

aerodynamic admittance function at non-dimensional frequencies of approx.  $10^{-1}$ . The large peak observed at this non-dimensional frequency could possibly be due to vortex-induced vibrations with a Strouhal number of 0.10. For a structure with geometrical dimensions as of the CAARC building, the Strouhal number may be in this region.

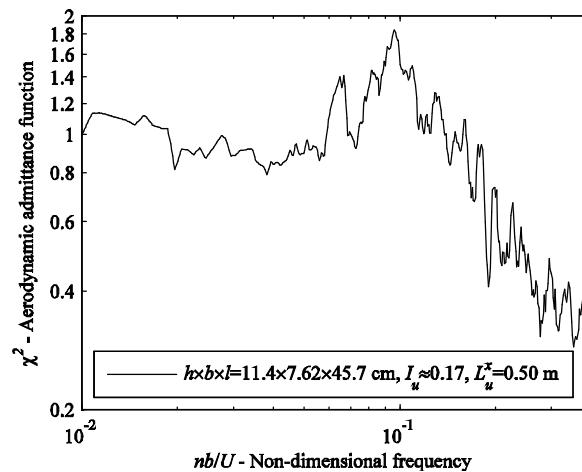


Figure 9. Aerodynamic admittance function for the CAARC building. Note that the frequency has been normalized with the lateral cross-wind dimensions  $b$  of the structure as this dimension is to a greater extent related to vortex shedding.

The application of the aerodynamic admittance function may especially be relevant for high-rise structures, which are generally constructed as slender structures, and may therefore have non-dimensional frequencies above  $10^{-1}$ , where the aerodynamic admittance function is below unity. As an example, the fundamental bending frequency may be estimated to  $n_1 = 46/h$  [7],  $n_1$  in [Hz] and  $h$  in [m], and by considering a dimensioning wind velocity of say 46 m/s, the non-dimensional frequency reduces to  $b/h$ . This means that for constructions with geometrical dimensions of  $b/h$  larger than  $10^{-1}$ , a reduction of the buffeting loads and resonant response predictions may potentially be enforced.

### Correlation of wind turbulence and surface pressure fluctuations

The lateral spatial correlations of the undisturbed wind and the fluctuating pressures, expressed mathematically by the co-spectrum, are given in Figure 10 and Figure 11 for the  $h \times b \times l = 5 \times 5 \times 170$  cm and  $h \times b \times l = 10 \times 10 \times 170$  cm structure, respectively. The spatial correlations are presented for three lateral separations of  $r_y = 0.05$  m, 0.15 m, and 0.30 m.

The upstream surface pressure correlation characteristics are found to be much similar to that of the along-wind turbulence components of the undisturbed wind, especially for separations comparable or larger than the associated length scale of the wind turbulence. This implies that surface pressure correlations along large line-like structures, such as long-span bridges, may very well be described appropriately by utilizing the correlation of along-wind turbulence components in the undisturbed air flow, as described by a modified exponential format; see Equation (4). The model framework also captures the reduced correlation at large separations, even for very small frequencies. The findings provide an additional verification of the key elements in the generic buffeting load model proposed in a previous paper [1].

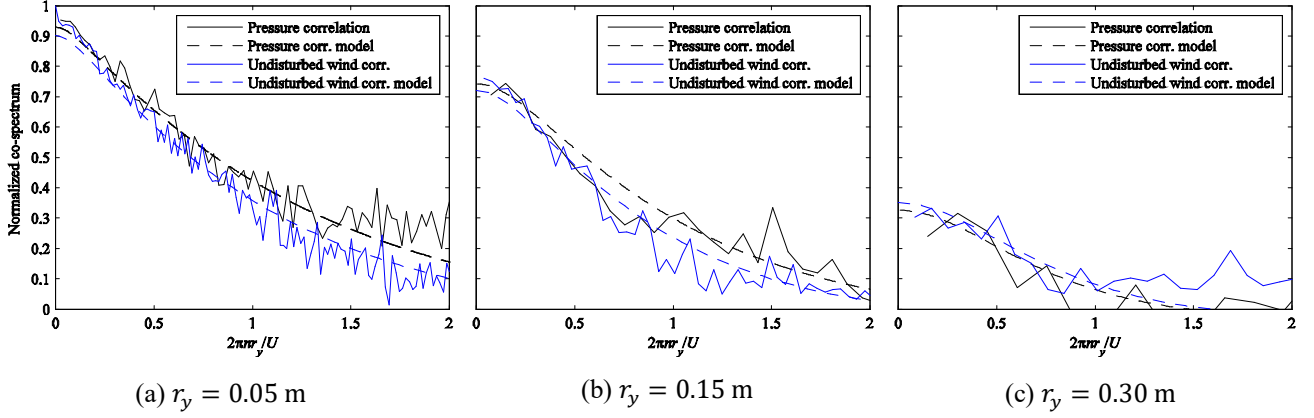


Figure 10. Normalized co-spectra of the undisturbed wind and surface pressure fluctuations for the  $h \times b \times l = 5 \times 5 \times 170$  cm model structure at lateral separations of  $r_y = 0.05$  m,  $0.15$  m, and  $0.30$  m. The dashed lines show the pressure correlation model given in Equation (4). For the pressure fluctuations, the following parameters were used:  $L = 1.10L_u^x = 0.55$  m and  $C_y = 3.4, 4.5,$  and  $8.0$ . For the undisturbed wind, the following parameters were used:  $L = 1.10L_u^x = 0.55$  m and  $C_y = 4.0, 5.3,$  and  $7.5$ .

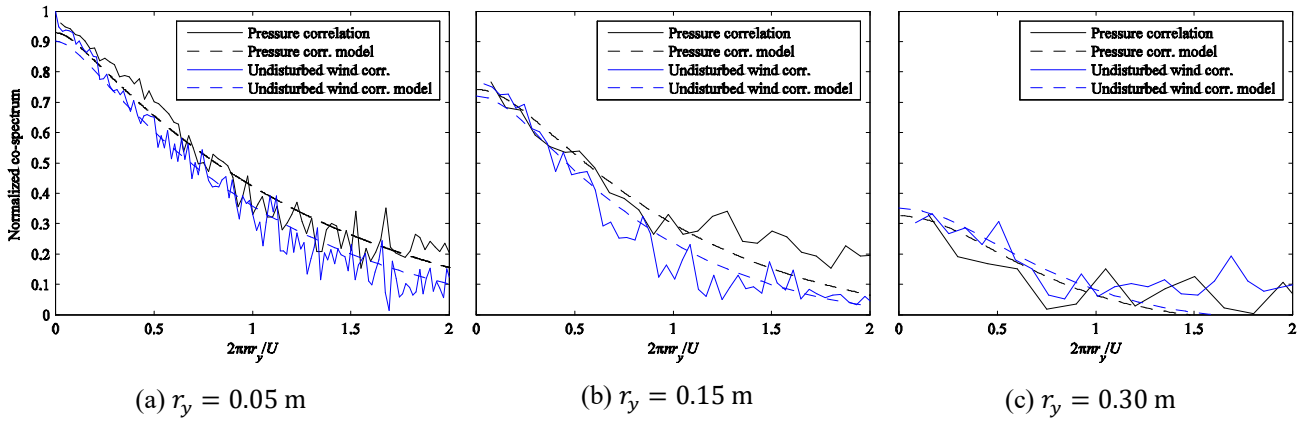


Figure 11. Normalized co-spectra of the undisturbed wind and surface pressure fluctuations for the  $h \times b \times l = 10 \times 10 \times 170$  cm model structure at lateral separations of  $r_y = 0.05$  m,  $0.15$  m, and  $0.30$  m. The dashed lines show the pressure correlation model given in Equation (4). For the pressure fluctuations, the following parameters were used:  $L = 1.10L_u^x = 0.55$  m and  $C_y = 3.4, 4.5,$  and  $8.0$ . For the undisturbed wind, the following parameters were used:  $L = 1.10L_u^x = 0.55$  m and  $C_y = 4.0, 5.3,$  and  $7.5$ .

It is noteworthy that the decay constants  $C_y$  increase as the lateral distance is increased. This has not been further investigated.

## CONCLUSION

The identified characteristics of upstream surface pressures generated by fluctuating winds allow for a more general understanding of the governing aerodynamic effects of relevance for buffeting load and response predictions. Especially the resonant response is of relevance as the full-scale natural frequencies of the slender constructions typically lie in a range where the aerodynamic admittance function is below unity. The outlined methodologies and results could potentially extend existing codified procedures, and are primarily useful in relation to buffeting load and response predictions for modern high-rise and long-span structures.

## ACKNOWLEDGEMENTS

The team at SOH Wind Engineering LLC in Burlington, Vermont, USA, is acknowledged for their great help with the tests of the CAARC building model.

The team at Svend Ole Hansen ApS is greatly acknowledged for their great help with the tests of the slender and point-like model structures and calculations of some aerodynamic admittance functions.

## REFERENCES

- [1] K. Hoffmann, R.G. Srouji and S.O. Hansen, 2016, "Buffeting loads on high-rise and long-span structures", *8th International Colloquium on Bluff Body Aerodynamics and Applications*, June 6. Boston, USA.
- [2] S.O. Hansen and C. Dyrbye, 1997, *Wind Loads on Structures*, John Wiley & Sons Ltd., Chichester, England.
- [3] A.G. Davenport, 1962, "The response of slender line-like structures to a gusty wind", *Proceedings of the Institution of Civil Engineers*, 23, 389-408.
- [4] S. Krenk, 1995, "Wind field coherence and dynamic wind forces", *Symposium on the Advances in Nonlinear Stochastic Mechanics*, Naess and Krenk (eds.), Kluwer Academic Publishers, Dordrecht.
- [5] T. von Kármán, 1948, "Progress in the statistical theory of turbulence", *Proceedings of the National Academy of Sciences of the United States of America*, 34, 530.
- [6] S.O. Hansen, 2013, "Vortex-induced vibrations – the Scurton number revisited", *Proceedings of the Institution of Civil Engineers – Structures and Buildings*, 166, 560-571.
- [7] Eurocode 1: Actions of structure - Part 1-4: General actions – Wind actions, 2005, CEN.